Evolutive differentiation between alga-and plant-type plastid terminal oxidase: study of plastid terminal oxidase PTOX isoforms in Marchantia polymorpha

Marine Messant, Ginga Shimakawa, François Perreau, Chikahiro Miyake, Anja Krieger-Liszkay

Evolutive differentiation between alga- and plant-type plastid terminal oxidase: study of plastid terminal oxidase PTOX isoforms in *Marchantia polymorpha*

Marine Messant[1,*], Ginga Shimakawa[1,*], François Perreau[2], Chikahiro Miyake[3], Anja Krieger-Liszkay[1,+]

[1]Institute for Integrative Biology of the Cell (I2BC), CEA, CNRS, Université Paris-Saclay, 91198, Gif-sur-Yvette cedex, France

[2]Institut Jean-Pierre Bourgin, INRAE, AgroParisTech, Université Paris-Saclay, 78000, Versailles, France

[3]Graduate School of Agricultural Science, Kobe University, 1-1 Rokkodai, Nada, Kobe 657-8501, Japan

*authors contributed equally

[+]Author for correspondence: Anja Krieger-Liszkay; e-mail anja.krieger-liszkay@cea.fr

Keywords: plastid terminal oxidase; *Marchantia polymorpha*; plastoquinone pool; chlororphyll fluorescence; P700 absorption

High lights

- MpPTOX isoforms belong to two different classes
- MpPTOX isoforms have a redundant function keeping the plastoquinone pool oxidized
- Actvity of the two isoforms differs depending on illumination conditions

Abbreviations

AOX, Alternative Oxidase; DCMU, 3-(3,4-dichlorophenyl)-1,1-dimethylurea; NDH; NADH dehydrogenase-like complex; NPQ; Non-Photochemical Quenching; PGR5 : Proton Gradient Regulation 5; PGRL1, PRG5-like protein; PIFT, Post-Illumination Fluorescence Transient; PQH_2, plastoquinol; PQ, plastoquinone; PS, Photosystem; PTOX, Plastid Terminal Oxidase

Abstract

The liverwort *Marchantia polymorpha* contains two isoforms of the plastid terminal oxidase (PTOX), an enzyme that catalyzes the reduction of oxygen to water using plastoquinol as substrate. Phylogenetic analyses showed that one isoform, here called MpPTOXa, is closely related to isoforms occurring in plants and some algae, while the other isoform, here called MpPTOXb, is closely related to the two isoforms occurring in *Chlamydomonas reinhardtii*. Mutants of each isoform were created in *Marchantia polymorpha* using CRISPR/Cas9 technology. While no obvious phenotype was found for these mutants, chlorophyll fluorescence analyses demonstrated that the plastoquinone pool was in a higher reduction state in both mutants. This was visible at the level of fluorescence measured in dark-adapted material and by post illumination fluorescence rise. These results suggest that both isoforms have a redundant function. However, when P700 oxidation and re-reduction was studied, differences between these two isoforms were observed. Furthermore, the mutant affected in MpPTOXb showed a slight alteration in the pigment composition, a higher non-photochemical quenching and a slightly lower electron transport rate through photosystem II. These differences may be explained either by differences in the enzymatic activities or by different activities attributed to preferential involvement of the two PTOX isoforms to either linear or cyclic electron flow.

1. **Introduction**

One of the most important events in the evolution of photosynthetic organisms has been the colonization of lands. Alboresi *et al*. [1] have highlighted the great diversity of protection mechanisms that allow photosynthetic organisms to face environmental conditions that could induce oxidative stress and destruction of the photosynthetic apparatus (photoinhibition) when more light is absorbed than needed for photosynthesis. All oxygenic phototrophs ranging from algae to plants have the following regulation mechanisms in common: photosynthetic control limiting electron transport at the level of the cytochrome b_6f complex when the pH in the lumen decreases below a certain threshold value [2]; mechanisms to dissipate excess energy in the antenna system, the so-called non-photochemical quenching (NPQ) [3]; the proton gradient regulation 5 (PGR5) and PGR5-like 1 (PGRL1) proteins having a supposed role in the cyclic electron flow [4-5]; the chloroplast NADPH dehydrogenase (NDH) complex involved in cyclic electron flow and in chlororespiration [6-7] as well as the so-called Mehler reaction (the water-water cycle) that occurs when photosystem I (PSI) reduces O_2 to the superoxide anion radical

which is then converted into O_2 and H_2O by detoxification enzymes [8]. Others, such as flavodiiron proteins (FLV) that reduce O_2 to H_2O at the acceptor side of PSI [9-10] have disappeared in angiosperms, but are present from cyanobacteria up to gymnosperms. Finally, some proteins have evolved over the time into separate subclasses such as the plastid terminal oxidase (PTOX).

PTOX oxidizes plastoquinol (PQH_2) and reduces O_2 to H_2O. It may play an important physiological role since the redox state of the plastoquinone (PQ) pool is a key point of photosynthesis regulation in many physiological conditions. In angiosperms, PTOX is often regarded in the literature as a "safety valve", allowing to avoid the over-reduction of PQ pool in conditions such as for example high light [11] or salt stress [12]. An increase of PTOX expression levels and of protein amounts have been observed upon exposure of plants to abiotic stress conditions like low or high temperature, drought etc. [13-14] Furthermore, PTOX is involved in carotenoid biosynthesis by maintaining PQ in its oxidized form [15-16]. In addition, PTOX acts as a terminal oxidase during chlororespiration [17] and in non-green plastids in etiorespiration [18] and chromorespiration [19-20]. Finally, PTOX is important in the first steps of chloroplast biogenesis, based on the publication by Wetzel *et al*. (1994) [15], highlighting that mutants have heteroplastidic cells.

Phylogenetic trees on PTOX evolution have been published previously focussing on amino acid sequences comparison with other oxidases [21-22]. Nawrocki *et al.* [23] has investigated the evolutionary relationship among PTOX isoforms in various photosynthetic organisms, which suggested that PTOX in angiosperms has been evolved along with the evolution from green algae to plants with several independent duplication events. The appearance of the ancestral protein is not clearly identified. Atteia and coworkers [24] hypothesized that the origin of PTOX predates primary endosymbiotic events, justifying its presence in the progeny of chlorophytes. Nevertheless, most articles agree that PTOX appears to diverge from its analogue, the mitochondrial alternative oxidase (AOX) that catalyzes the oxidation of ubiquinol by reducing O_2 to H_2O. AOXs are non-heme diiron carboxylate enzymes with six well conserved iron binding sites. It has been shown that this catalytic site including the ligands is conserved in PTOX [25] but PTOX diverges from AOX by insertion of amino acids conserved in all PTOX-containing photosynthetic organisms.

Characterization of PTOX activity *in vivo* has been mainly conducted in angiosperms by the characterization of *immutans* and *ghost* mutants in *Arabidopsis thaliana* [15,26-28] and *Solanum lycopersicum* [29], respectively. These mutants are known to have a variegated

phenotype which is more important when exposed to increasing light intensities[30]. In addition, PTOX activity has been characterized *in vivo* in the green alga *Chlamydomonas reinhartii* using a mutant affected in the isoform PTOX2 (*Crptox2*). Houilles-Vernes *et al.* [31] have highlighted its involvement in chlororespiration. *Crptox2* shows an over-reduction of PQ pool and is also affected in redistributing light excitation energy between photosystem II (PSII) and PSI (the so-called state transition). Using a single mutant of the cytochrome b_6f complex as well as a double mutant of both cytochrome b_6f and PTOX2, they concluded that PTOX2 is the major oxidase used to reoxidize PQ pool compared to PTOX1 in *C. reinhartii*. *Crptox2* did not exhibit a defect in carotenoid contents and did not show a variegation phenotype such as *immutans* or *ghost*. Houille-Vernes and coworkers concluded that PTOX1 is sufficient for regenerating oxidized PQ for phytoene desaturase while being less active than PTOX2 in controlling the redox poise of PQ pool during photosynthesis. No PTOX1 mutant of *C. reinhartii* has been characterized so far.

Liverworts can be regarded as the oldest living land plants or at least the land plants which have kept the most ancestral characters, among them *Marchantia polymorpha* has been used as a model with the sequencing of its genome and the development of genetic tools in order to better understand the evolution of land plants [32-33]. Here we demonstrate that the two *M. polymorpha* PTOX isoforms are phylogenetically significantly different and representative of algal- and angiosperm-type of PTOX respectively, and if they differ in their activity by using mutants affected in one of the isoforms. First, we focussed on PTOX evolution through the green lineage using *in silico* approaches. Then, mutation of both proteins independently allowed us to highlight the partial redundancy of these proteins *in vivo* by performing mainly chlorophyll fluorescence analyses.

2. **Materials and Methods**

2.1. Phylogenetic analysis

31 amino acid sequences of PTOX and AOX in oxygenic phototrophs were aligned using Muscle [34], and then the extra N- and C-terminal regions were removed based on the comparison to cyanobacterial PTOX sequences. Thereafter, gaps in the alignment were removed using Gap Squeeze

(https://www.hiv.lanl.gov/content/sequence/GAPSTREEZE/gap.html) with 50% of gap tolerance. The resulting sequences were compared using Muscle for building up phylogenetic trees (Supplementary Material Fig. S1). The amino acid sequences of PTOX and AOX were obtained from CyanoBase (Glo, gll0601; Ana, Anacy_4546; Nos, all2096), National Center for Biotechnology Information (Coc, XP_005649673; Tha a, XP_002293901; Tha b, XP_002296917), Joint Genome Institute (Ost a, Ot11g01620; Ost b, Ot16g00910; Chl 1, Cre07.g350750; Chl 2, Cre03.g172500; Chl A, Cre09.g395950; Vol 1, Vocar.0011s0051; Vol 2, Vocar.0015s0153; Ory, Os04g57320; Zos, Zosma182g00520; Zea, Zm00008a005994; Nan a, 587833; Nan b, 605717; Pha a, 29275; Pha b, 41170; Cya 1, XM_005536341; Cya 2, XM_005536340), *Klebsormidium nitens* NIES-2285 genome project (Kle a, kfl00205_0040: Kle b, kfl00009_0280), MarpolBase (Mar a, Mapoly0050s0020; Mar b, Mapoly0003s0157), FernBase (Azo a, Azfi_s0009.g011680; Azo b, Azfi_s0070.g036665; Sal, Sacu_v1.1_s0132.g022138), and TAIR (Ara, AT4G22260; Ara A, AT3G22370).

The evolutionary history was inferred by using the Maximum Likelihood method [35]. The tree with the highest log likelihood (-8225.18) is shown. The percentage of trees in which the associated taxa clustered together is shown next to the branches. Initial trees for the heuristic search were obtained automatically by applying Neighbor-Join and BioNJ algorithms[36] to a matrix of pairwise distances estimated using a JTT model, and then selecting the topology with superior log likelihood value. The tree is drawn to scale, with branch lengths measured in the number of substitutions per site. Evolutionary analyses were conducted in MEGA X [37].

2.2. Material

A male accession of *Marchantia polymorpha*, Takaragaike (Tak)-1 and the mutants were asexually cultured on one-half-strength Gamborg's B5 agar medium [38] under a light–dark cycle (16 h–light, 22°C, 120 µmol photons m^{-2} s^{-1}, white fluorescent lamp/8 h–dark, 20°C). For biochemical and physiological measurements, 3–4 week–old thalli were used.

2.3. Genome editing by CRISPR/Cas9 system

The PTOX mutants of *M. polymorpha* were prepared by CRISPR/Cas9-based targeted mutagenesis [39]. The target regions (*ptoxa.1*, TTACACATGTACGAGAGCTT; *ptoxb.1*,

CCAGGTTGTGAGTCCCAACC; *ptoxb.2*, AAGCACCTTGGTGGATTCT) were introduced into the Gateway entry vector pMpGE_En03, and finally included in the destination vector pMpGE010 and pMpGE011. Thalli of *M. polymorpha* were infected with *Rhizobium radiobactor* C58C1 (GV2260) transformed with the resulting plasmids, and the transformants were selected on half-strength Gamborg's B5 agar medium supplemented with hygromycin or chlorsulfuron[40]. The genome DNA was extracted from the thalli of mutants, and the mutations were confirmed by DNA sequencing (Supplementary Material Fig. S2). The mutants *Δptoxa.1* and *Δptoxb.1* were mainly used in this study as *Δptoxa* and *Δptoxb*. We confirmed the same phenotype of *Δptoxb.2* as *Δptoxb.1* by chlorophyll fluorescence measurements (Supplementry Material Fig. S3).

2.4. Pigment analysis

Liquid chromatography-UV-absorption analysis was conducted using a HPLC column (Uptisphere Strategy C18-HQ 250 × 3 mm 3 µm, Interchim, Montluçon, France) with a liquid chromatography chain HPLC/UV (Shimadzu, Tokyo, Japan), consisting of two pumps (LC-20AD), a sample manager (SIL-20AC HT), a column oven (CTO-20A) and an UV diode array detector (UVSPD-M20A) with a flow of 0.5 mL min^{-1}. The mobile phase A was composed of 10% water and 90% acetonitrile with 0.5% acetic acid and the mobile phase B was ethyl acetate with 0.5% acetic acid. The elution gradient was as follows: initially 10% B, 1 min 10% B; 25 min 95% B. Then the column was equilibrated to initial conditions for 15 min. Absorbance was monitored at 450 nm. Peak areas were normalized by known absorption factors for each compound at 450 nm, and amounts of each pigment were calculated by normalization to chlorophyll a.

2.5. Chlorophyll fluorescence analysis

Chlorophyll *a* fluorescence was measured in 5 min dark-adapted thalli using an Imaging-PAM (Fig. 2 and Supplementary Material Fig. S3A-C, and S4) or a Dual-PAM-100 fluorometer (Fig. 3 and 4, and Supplementary Material Fig. S3D) (Walz, Effeltrich, Germany). Fluorescence parameters during illumination with blue actinic light (230 µmol photons $m^{-2}s^{-1}$) and recovery curves were measured after the determination of

F_o and F_m parameters. F_m and F_m' were determined using saturating flashes (10,000 µmol photons $m^{-2}s^{-1}$, duration 300 ms): F_o, minimum and F_m, maximum fluorescence in a dark-adapted sample; F_m', maximum fluorescence and F′, fluorescence emission from a light-adapted sample [41]. Post-Illumination Fluorescence Transient (PIFT) was monitored in the dark after exposure to actinic red light (400 µmol photons $m^{-2}s^{-1}$) for 10 min. When indicated, far-red light was given. Quantum yield of photochemical energy conversion in PSII, Y(II), and NPQ were determined as $(F_m'-F')/F_m'$ and $(F_m-F_m')/F_m'$, respectively. Electron transport rate through PSII was calculated as the product of Y(II) multiplied with photon flux density of red actinic light, the sample absorptance, and the ratio of the absorbance by PSII to that by both PSI and PSII [42]; we used 0.8 and 0.5, respectively, as these absorptance values which had been determined for leaves.

2.6. P700 measurement

P700 absorbance was measured using a Dual-PAM-100 fluorometer [43] (Walz, Effeltrich, Germany). Near-infrared measuring lights (830 and 870 nm) were applied to measure the transmittance of oxidized P700 ($P700^+$). Five minutes dark-adapted thalli were exposed to actinic light and far-red light for 15s. Then, a saturating flash was given in the presence of far-red light after switching off the light. First, this experiment was done on intact thalli which were then immersed for 5 min in 100 µM 3-(3,4-dichlorophenyl)-1,1-dimethylurea (DCMU) or in a combination of DCMU and 500 µM methylviologen.

2.7. Immunoblots

Thalli were grinded in 50 mM HEPES pH 7.6. The extract was filtered through cheese, centrifuged at 4000g, the pellet was resuspended in 50 mM HEPES pH 7.6, the chlorophyll concentration was determined and this membrane fraction was used for analysis by SDS-PAGE (10% acrylamide) and immunoblotting. Proteins were blotted onto nitrocellulose membrane. Labelling of the membranes with anti-PGR5, anti-NDH-B and anti-RbcL (Agrisera, Vännäs, Sweden) was carried out at room temperature in 1x PBS (50 mM Tris-HCl pH 7.6, 150 mM NaCl), 0.1% Tween 20 and 1% non-fat powder milk). After washing, bound antibodies were

revealed with a peroxidase-linked secondary anti-rabbit antibody (Agrisera, Vännäs, Sweden) and visualized by enhanced chemiluminescence. PTOX antibodies raised against the proteins from Arabidopsis (gift from Marcel Kuntz, CEA Grenoble) and *Chlamydomonas reinhardtii* (gift from Xenie Johnson, CEA Cadarache) did not reveal bands in *Marchantia polymorpha*.

3. **Results**

Marchantia polymorpha contains two PTOX isoforms (MpPTOXs) that differ significantly in their sequences. The study of PTOX evolution has so far been limited to the comparison of their protein sequences with those of AOXs. However, the more recent evolution of different PTOX isoforms is just as interesting. Sequence comparison shows that MpPTOXa is closely related to PTOX of angiosperms that usually contain only one isoform, while MpPTOXb is more similar to PTOX isoforms found in the green alga *Chlamydomonas reinhardtii* (CrPTOXs). Since the PTOX isoform of *Arabidopsis thaliana* has been highlighted first, the isoforms resembling to it were defined here as "PTOXa" and the other isoforms as "PTOXb". MpPTOXa shows 96% identity with PTOX in *Arabidopsis thaliana* (AtPTOX), while MpPTOXa and MpPTOXb share only 53% identity. Since the two MpPTOX isoforms are so different in respect to their sequence homology, it can be hypothesized that these proteins have different physiological functions. A closer look at the sequences revealed that MpPTOXb and CrPTOXs (hereafter defined as "alga-type PTOX") are larger than MpPTOXa and AtPTOX (hereafter defined as "plant-type PTOX"; Fig. 1A). CrPTOX1 and CrPTOX2 are composed of 471 and 416 amino acid residues. MpPTOXb has 497 amino acid residues while MpPTOXa and AtPTOX contain only 376 and 352 ones (Supplementary Material, Figure S1).

31 amino-acid sequences of PTOX isoforms were investigated in a variety of photosynthetic organisms, including cyanobacteria, algae, and land plants. Although the C-terminal parts of the proteins are not particularly well conserved between these isoforms, the longer N-terminal part is mostly recognized in alga-type PTOX. Plant-type PTOX seems to have lost a part of the sequence between the transit peptide and the conserved motif containing the catalytic site (Fig. 1A), resulting in the shorter primary structures, although there are some exceptions such as *Zea mays* and *Nannochloropsis oceanica*. A phylogenetic tree including cyanobacterial PTOX, alga-type PTOX, plant-type PTOX, and AOX was built (Fig. 1B) based on the amino acid sequence alignment in the largely conserved region containing the catalytic

site (the part "Fe-Fe" in Fig. 1A) among PTOX isoforms in a variety of photosynthetic organisms, clearly showing the three different PTOX groups. Several amino acid residues around the catalytic site are highly conserved in alga- and plant-type PTOX (Supplementary Material Fig. S1). The green alga *Coccomyxa subellipsoidea* has one PTOX belonging to the alga-type. *Chlamydomonas reinhardtii* and *Volvox carteriv* have two PTOX isoforms, both belonging to the alga-type. The other green alga *Ostreococcus tauri* has both alga- and plant-type PTOX isoforms. Seed plants are proposed to be evolved from green algae through charophytes, bryophytes (liverworts, mosses, and hornworts), and pteridophytes (ferns), termed as photosynthetic green lineage [44]. Like in *Ostreococcus tauri* both alga- and plant-type PTOX isoforms are conserved in the charophyte alga *Klebsormidium nitens*, the liverwort *Marchantia polymorpha*, and the fern *Azolla filiculoides*, but alga-type one is lost in the fern *Salvinia cucullata* and in all angiosperms (Fig. 1B). In contrast to the green lineage, photosynthetic red lineage is defined as having evolved from red algae to secondary algae such as eustigmatophytes and diatoms[44]. The red alga *Cyanidioschyzon merolae* has two PTOX isoforms, both of which are closer to the alga-type ones, but the eustigmatophyte alga *Nannochloropsis oceanica* and two diatoms *Phaeodactylum tricornutum* and *Thalassiosira pseudonana* have both, alga- and plant-type PTOX (Fig. 1B).

Since the two MpPTOX isoforms are so different in respect to their sequence homology, it can be hypothesized that these proteins have different physiological functions. To characterize the physiological role of the two PTOX isoforms *in vivo*, *M. polymorpha* has been chosen since it has one PTOX belonging to the plant-type and another one of the alga-type enzyme, and its position in the evolution of the green line is intermediate between green algae and plants [33]. The mutants deficient in MpPTOXa and MpPTOXb, named hereafter Δ*ptoxa* and Δ*ptoxb*, were constructed using CRISPR/Cas9-genome editing system [39]. The specific regions to MpPTOXa and MpPTOXb were determined as the target site for CRISPR/Cas9. The *Marchantia* transformants were generated by the infection of Agrobacterium containing binary vectors with young thalli in the presence of antibiotics (see "Materials and Methods"). The gemma from the transformants were cultured on agar plates with the antibiotics, and finally the frameshift mutation in the target regions were confirmed by DNA sequencing (Supplementary Material Fig. S2). Concerning that the mutation occurred at the later part of the gene in the mutant Δ*ptoxb* (Δ*ptoxb.1*), we constructed another line (Δ*ptoxb.2*) to confirm that the phenotype was due to the mutation of PTOXb (Supplementary Material Fig. S2 and S3). Similar

to *Crptox2*, no variegation phenotype such as *immutans* or *ghost* was seen in both Δ*ptoxa* and Δ*ptoxb* mutants.

In order to characterize the role of PTOX on photosynthetic electron transport, measurements of chlorophyll fluorescence upon illumination and dark recovery were carried out. As shown in Fig. 2, upon illumination with actinic light Δ*ptoxb* showed a lower fluorescence level during saturating pulses while Δ*ptoxa* was very similar to Tak-1 (wild type). When the actinic light was switched off, fluorescence levels in mutants decreased below the F_o level, more significantly for Δ*ptoxb* than for Δ*ptoxa*. This can be either caused by a higher level of NPQ leading to a quenching of F_o or chlororespiratory activity resulting in a higher reduction state of PQ pool, Q_B and Q_A in the dark giving rise to a higher fluorescence level. In this case, dark adaptation of the material prior to the fluorescence measurement does not assure that all reaction centers are in the "open state".

One way to determine chlororespiratory activity is to follow the so-called Post-Illumination Transient Fluorescence (PIFT) rise. Illumination with actinic light for a given time leads to the production of NADPH and ATP that can be consumed in the dark leading to a transient reduction of the PQ pool, Q_B and Q_A. Figure 3 shows after previous illumination in the dark a strong increase in the fluorescence level (PIFT) in both mutants detected using low intensity measuring light. Applying far-red light removed the PIFT, confirming the high reduction state of the PQ pool in both mutants.

If one calculated F_v/F_m values using dark-adapted material and without taking into account that the F_o may be not correct, one obtains values for F_v/F_m being 0.56 ± 0.04 for Δ*ptoxa* and 0.61 ± 0.04 for Δ*ptoxb* (n = 6). If these values were determined after far-red light illumination, 0.69 ± 0.01 and 0.71 ± 0.01 were obtained for Δ*ptoxa* and Δ*ptoxb* (n = 6), similar to those measured for Tak-1. In the literature, the F_v/F_m value in Tak-1 was determined to be approximately 0.8 [45], but, when determined with an Imaging-PAM as done for the data shown in Fig. 2, a lower value was determined even when higher plants like *Arabidopsis thaliana* were used. This lower value is caused by a too high intensity of the measuring light in the Imaging-PAM system.

Next, we measured NPQ and the electron transport rate as a function of actinic light intensity (Fig. 4). Δ*ptoxb* showed a lower electron transport rate and a higher NPQ while Δ*ptoxa* behaved like Tak-1. Pigment analysis showed that the amounts of certain carotenoids such as neoxanthin and violaxanthin were slightly larger in Δ*ptoxb* (Fig. 5). The increase in pigment content of the violaxanthin pool may explain the stronger NPQ found in this genotype. It may also indicate that Δ*ptoxb* is more stressed than Δ*ptoxa* or Tak-1, leading to a lower electron

transport rate. However, no higher susceptibility to photoinhibition was observed in Δ*ptoxb* (Supplementary Material Fig. S4).

When the PQ pool is more oxidized in the dark, it is expected that $P700^+$ is accumulating to a higher level in response to the illumination at a given light intensity. As can be seen in Figure 6, more $P700^+$ accumulated in Tak-1 upon illumination with either actinic or far-red light. Both mutants showed the same lower level of P700 oxidation suggesting that PQ pool was more reduced, if we consider that there was no PSI acceptor side limitation thanks to the presence of FLV [45]. There are nevertheless striking differences between Δ*ptoxa* and Δ*ptoxb*. Upon illumination with actinic light that excites both photosystems and favours linear electron flow, the oxidation of P700 was delayed in Δ*ptoxa* compared with Δ*ptoxb*, especially at the initial rise. This seems to indicate that the PQ pool was more reduced in Δ*ptoxa*, suggesting a higher activity of this enzyme. However, when illuminated with far-red light that excites preferentially PSI and favours cyclic electron flow, P700 was faster oxidized in Δ*ptoxa* than in Δ*ptoxb*. To show the electron donation to P700 and the reduction state of the PQ pool in the absence of electron input from PSII, we added DCMU, an inhibitor of PSII blocking the Q_B-binding pocket. The re-reduction of $P700^+$ after far-red illumination was much faster in Δ*ptoxa* than in Δ*ptoxb* and Tak-1, with Δ*ptoxb* being slightly faster than Tak-1 (Fig. 7). This indicates again a higher reduction state of the PQ pool in Δ*ptoxa*. In the absence of inhibitors, the re-reduction of $P700^+$ after far-red illumination was slightly faster in both mutants than in Tak-1. As expected, addition of the electron acceptor methylviologen together with DCMU abolished the differences between the mutants and Tak-1 (Supplementary Material Fig. S5). Immunoblots probing for NDH and PGR5 showed an increase in the amount of NDH in Δ*ptoxa* and of PGR5 in both, Δ*ptoxa* and Δ*ptoxb*.

4. **Discussion**

Here, we categorized PTOX isoforms in oxygenic phototrophs into three different groups (Fig. 1): cyanobacterial, alga-type, and plant-type PTOXs. Based on the present phylogenetic analysis, two different types of PTOX isoforms had been inherited to basal land plants from green algae like *Ostreococcus tauri* that is often described as one of the ancient members of the photosynthetic green lineage [46]. Both alga- and plant-type PTOXs are conserved in most basal land plants, while angiosperms have lost the alga-type PTOX. Also, the fern *Salvinia cucullata* has only a plant-type PTOX (Fig. 1B), and another fern, *Azolla filiculoides*, lost a conserved ligand of the non-heme diiron center, most probably leading to the loss or alteration in the

catalytic activity in its alga-type PTOX (Supplementary Material Fig. S1). These facts suggest that alga-type PTOX are already not functional in some pteridophytes. Both plant-type and alga-type PTOX are also found in secondary algae that are supposed to be derived from red algae in photosynthetic red lineage (Fig. 1B). In this study, we show that the red alga *Cyanidioschyzon merolae* has only two isoforms of alga-type PTOX. This may not be the case for all red algae and improved open genome sources of red algae may uncover the red algae species having both alga- and plant-type PTOX isoforms in near future. The appearance of the ancestral protein for PTOX has not been identified to date. However, many studies based on genomic sequence analysis seem to favor the hypothesis of PTOX acquisition during the primary endosymbiotic event, suggesting that this protein appeared much earlier than the eukaryotic lineage [21-22,24,47]. The question is when these alga- and plant-type PTOXs had been separated in the evolutionary history of photosynthetic organisms. It can be speculated that a single protein has been duplicated in eukaryotic algae, finally resulting in alga- and plant-type PTOXs, if we consider that cyanobacterial PTOX is closer to plant-type PTOX but can be clearly distinguished from both alga- and plant-type PTOXs. Interestingly, most of alga-type PTOX isoforms show longer N-terminal regions, resulting in bigger size of proteins (Fig. 1A and Supplementary Material Fig. S1). In addition, some amino acid residues are specifically conserved in each type of PTOX even in the motif containing catalytic sites (Supplementary Material Fig. S1), reflected also in the phylogenetic tree (Fig. 1B). Differences in enzymatic activities of these different types of PTOX remain to be characterized in future, possibly uncovering why angiosperms had lost alga-type PTOX during the evolutionary history.

The results shown here (Figs. 2, 3, 6, 7) indicate that both MpPTOX isoforms have redundant functions and are both important for controlling the redox state of the PQ pool. Especially the PIFT showing the slow electron donation to the PQ pool via the NDH complex during chlororespiration is similar in both mutants. However, there are small differences when comparing Δ*ptoxa* and Δ*ptoxb*. Δ*ptoxa* shows no difference in electron transport rate and NPQ compared with Tak1, whereas in Δ*ptoxb* the electron transport rate is lower while NPQ is higher. The lower electron transport rate and the higher NPQ and violaxanthin amount in Δ*ptoxb* suggest that this mutant is slightly stressed although no obvious phenotype was visible. *Crptox2* mutant showed a lower fitness when cells were grown under phototrophic conditions and was more susceptible to photoinhibition [31]. In addition, *Crptox2* was affected in the state transition being preferentially in state 2. In contrast, Δ*ptoxb* in *M. polymorpha* showed neither signs of a defect in the state transition nor a higher susceptibility to high light (Supplementary

Material Fig. S4) suggesting that the plant-type MpPTOXa could compensate better for the absence of MpPTOXb than it was the case in *C. reinhardtii* possessing only two alga-type isoforms. In respect to carotenoid synthesis MpPTOXb seems to replace perfectly MpPTOXa since the absence of MpPTOXa did not alter the carotenoid composition neither induced a variegated phenotype as described in angiosperms for *immutans* and *ghost*.

P700 measurements show that the isoform MpPTOXa is more efficient in keeping the PQ pool oxidized since the oxidation of $P700^+$ in actinic light was retarded in Δ*ptoxa* compared with Δ*ptoxb* (Fig. 6). However, under illumination with far-red light the opposite was observed with slower P700 oxidation in Δ*ptoxb* than in Δ*ptoxa*. Actinic light drives mainly reduction of the PQ pool by linear electron transport, while far-red light oxidizes the PQ pool and may also favour PQ reduction by cyclic electron flow. This leads us to hypothesize that PTOXa is more active in linear electron transport and PTOXb more in cyclic electron transport. This different behaviour of the PTOX isoforms at the different light qualities can be rationalized by different enzymatic properties, with MpPTOXb having a higher affinity (low K_m-value) for PQH_2 but a lower V_{max} than MpPTOXa. This would make MpPTOXa the more efficient enzyme keeping the PQ pool oxidized under conditions favouring linear electron flow. The proposition of a high activity of MpPTOXa is supported by the fact that, in the presence of DCMU, the reduction of $P700^+$ is accelerated in Δ*ptoxa* (Fig. 7). However, the amount of the NDH complex is also increased in Δ*ptoxa* (Fig. 8), and a higher chlororespiratory activity may also explain the higher reduction state of the PQ pool in this mutant. Since cyclic electron flow in far-red light is expected to be relatively low, the reduction state of the PQ pool may also be relatively low and MpPTOXb may become under these conditions highly efficient to keep the PQ pool oxidized. Alternatively, the two PTOX isoforms may be heterogeneously distributed within the thylakoid membrane. MpPTOXb may be preferentially associated with supercomplexes involved in cyclic flow composed of PSI, ferredoxin, cytochrome b_6f and a putative ferredoxin quinone reductase possibly linked to PGR5 and PGRL1 [48-49] while MpPTOXa may be preferentially associated with components of linear electron flow. A third possibility to explain the different behaviour of the two mutants may simply be a difference in the protein level of the two isoforms.

Both mutants have a higher amount of PGR5 (Fig. 8), indicating that the loss of a part of PTOX activity triggers the accumulation of higher amounts PGR5 and likely increases the capacity for cyclic electron transport. Cyclic electron transport may be important in these

mutants to compensate for a reduction of the PTOX-dependent chlororespiratory activity and to keep the size of the proton motive force.

PTOX activity may also be regulated as a function of the physiological state of the chloroplast. Stepien and Johnson [12] have demonstrated that plant PTOX is localized under control conditions at the stroma lamellae while it is localized at the grana stacks under salt stress in the halophile *Eutrema salsugineum*. Furthermore, it has been shown that AtPTOX could be found partially in a soluble protein fraction and in a membrane-associated fraction. The strength of the membrane association of AtPTOX was shown to depend on the proton motive force [13,50]. A difference between plant-type and alga-type PTOX may lie in the strength of the membrane association. Nawrocki and co-workers [23] carried out a modelling of the structure of CrPTOX2 based on the x-ray structure of AOX from *Trypanosoma brucei* (TbAOX)[51]. Shiba and coworkers [51] proposed that two alpha helices upstream of the catalytic site of TbAOX are involved in the anchoring to the inner mitochondrial membrane. According to the calculation by Nawrocki et al. [23] the amphipathic helices of CrPTOX dock to a depth of approximately 8Å into the membrane. They suggest that the N-terminal extension in CrPTOX contributes to the interaction of the two monomers of the protein. We propose here that the increase in length may as well strengthen the association of the protein to the upper membrane leaflet. Further studies are needed to investigate the difference in plant-type and alga-type PTOX regarding their attachment to the membrane and differences in the regulation of the activity of these isoforms.

Acknowledgements

We thank Dr. Kimitsune Ishizaki (Kobe University, Japan) for kindly giving us the Tak-1 strain. The I2BC and the IJPB benefit from the support of Saclay Plant Sciences-SPS (ANR-17-EUR-0007) and the I2BC from the French Infrastructure for Integrated Structural Biology (FRISBI) ANR-10-INSB-05. This work has benefited from the support of IJPB's Plant Observatory technological platforms. G.S. is supported by a JSPS oversea research fellowship (201860126).

References

[1] A. Alboresi, M. Storti, T. Morosinotto, Balancing protection and efficiency in the regulation of photosynthetic electron transport across plant evolution. New. Phytol. 221 (2018) 105-109.

[2] C. Foyer, R. FurbanK, J. Harbinson, P. Horton, The mechanisms contributing to photosynthetic control of electron transport by carbon assimilation in leaves. Photosynth. Res. 25 (1990) 83-100.

[3] P. Müller, X.P. Li, K.K. Niyogi, Non-photochemical quenching. A response to excess light energy. Plant Physiol. 125 (2001) 1558-1566.

[4] Y. Munekage, M. Hojo, J. Meurer, T. Endo, M. Tasaka, T. Shikanai, PGR5 is involved in cyclic electron flow around photosystem I and is essential for photoprotection in *Arabidopsis*. Cell 110 (2002) 361-371.

[5] M. Suorsa, F. Rossi, L. Tadini, M. Labs, M. Colombo, P. Jahns, M. M. Kater, D. Leister, G. Finazzi, E.M. Aro, R. Barbato, P. Pesaresi, PRG5-PGRL1-dependant cyclic electron transport modulates linear electron transport rate in *Arabidopsis thaliana*. Mol. Plant 9 (2015) 271-288.

[6] P. Bennoun, Evidence for a respiratory chain in the chloroplast. Proc. Natl. Acad. Sci. U. S. A. 79 (1982) 4352-4356.

[7] G. Peltier, E.M. Aro, T. Shikanai, NDH-1 and NDH-2 plastoquinone reductases in oxygenic photosynthesis. Annu. Rev. Plant Biol. 67 (2016) 55-80.

[8] K. Asada, The water-water cycle as alternative photon and electron sinks. Philos. Trans. R. Soc. Lon. B. Biol. Sci. 355 (2000) 1419-1431.

[9] Y. Helman, D. Tchernov, L. Reinhold, M. Shibata, T. Ogawa, R. Schwarz, I. Ohad, A. Kaplan, Genes encoding A-type flavoproteins are essential for photoreduction of O_2 in cyanobacteria. Curr. Biol. 13 (2003), 230-235.

[10] A. Alboresi, M. Storti, L. Cendron, T. Morosinotto, Role and regulation of class-C flavodiiron proteins in photosynthetic organisms. Biochem. J. 476 (2019) 2487-2498.

[11] C. Laureau, R. De Paepe, G. Latouche, M. Moreno-Chacon, G. Finazzi, M. Kuntz, G. Cornic, P. Streb, Plastid Terminal Oxidase (PTOX) has the potential to act as a safety valve for excess excitation energy in the alpine plant species *Ranunculus glacialis* L. Plant Cell. Environ. 36 (2013) 1296-1310.

[12] P. Stepien, G.N. Johnson, Plastid terminal oxidase requires translocation to the grana stacks to act as a sink for electron transport. Proc. Natl. Acad. Sci. U. S. A. 115 (2018) 9634-9639

[13] K. Feilke, P. Streb, G. Cornic, F. Perreau, J. Kruk, A. Krieger-Liszkay, Effect of Chlamydomonas plastid terminal oxidase 1 expressed in tobacco on photosynthetic electron transfer. Plant J. 85 (2016) 219-228.

[14] G.N. Johnson, P. Stepien, Plastid terminal oxidase as a route to improving plant stress tolerance: Known knowns and known unknowns. Plant Cell. Physiol. 57 (2016) 1387-1396.

[15] C. M. Wetzel, C.Z. Jiang, L.J. Meehan, D.F. Voytas, S.R. Rodermel, Nuclear-organelle interactions: the immutans variegation mutant of Arabidopsis is plastid autonomous and impaired in carotenoid biosynthesis. Plant J. 6 (1994) 161-175.

[16] P. Carol, D. Stevenson, C. Bisanz, J. Breitenbach, G. Sandmann, R. Mache, G. Coupland, M. Kuntz, Mutations in the *Arabidopsis* gene IMMUTANS cause a variegated phenotype by inactivating a chloroplast terminal oxidase associated with phytoene desaturation. Plant Cell 11 (1999) 43-55.

[17] G. Peltier, L. Cournac, Chlororespiration. Annu. Rev. Plant Biol. 53 (2002) 523-550.

[18] S. Kambakam, U. Bhattacharjee, J. Petrich, S. Rodermel, PTOX mediates novel pathways of electron transport in etioplasts of *Arabidopsis*. Mol. Plant 9 (2016) 1240-1259.

[19] M. Renato, I. Pateraki, A. Boronat, J. Azcón-Bieto, Tomato fruit chromoplasts behave as respiratory bioenergetic organelles during ripening. Plant Physiol. 166 (2014) 920-933.

[20] M. Grabsztunowicz, P. Mulo, F. Baumann, R. Mutoh, G. Kurisu, P. Sétif, P. Beyer, A. Krieger-Liszkay, Electron transport pathways in isolated chromoplasts from *Narcissus pseudonarcissus* L. Plant J. 99 (2019) 245-256.

[21] A.E. McDonald, S. Amirsadeghi, G.C. Vanlerberghe, Prokaryotic orthologues of mitochondrial alternative oxidase and plastid terminal oxidase. Plant Mol. Biol. 53 (2003) 865-876.

[22] P.M. Finnegan, A.L. Umbach, J.A. Wilce, Prokaryotic origins for the mitochondrial alternative oxidase and plastid terminal oxidase nuclear genes. FEBS Lett. 555 (2003) 425-430.

[23] W.J. Nawrocki, N. J. Tourasse, A. Taly, F. Rappoport, F.A. Wollman, The plastid terminal oxidase: its elusive function points to multiple contributions to plastid physiology. Annu. Rev. Plant Biol. 66 (2015) 49-74.

[24] A. Atteia, R. van Lis, J.J. Van Hellemond, A.G. Tielens, W. Martin, K. Henze, Identification of prokaryotic homologues indicates an endosymbiotic origin for the alternative oxidases of mitochondria (AOX) and chloroplasts (PTOX). Gene. 330 (2004) 143-148.

[25] A. Fu, S. Park, S. Rodermel, Sequences required for the activity of PTOX (*IMMUTANS*), a plastid terminal oxidase. J. Bio. Chem. 280 (2005), 42489-42496.

[26] L. Meehan, K. Harkins, J. Chory, S. Rodermel, Lhcb transcription is coordinated with cell size and chlorophyll accumulation (Studies on fluorescence-activated, cell-shorter-purified single cells from wild-type and immutans *Arabidopsis thaliana*). Plant Physiol. 112 (1996) 953-963.

[27] C.M. Wetzel, S.R. Rodermel, Regulation of phytoene desaturase expression is independent of leaf pigment content in *Arabidopsis thaliana*. Plant Mol. Biol. 37 (1998) 1045-1053.

[28] D. Wu, D.A. Wright, C. Wetzel, D.F. Voytas, S. Rodermel, The IMMUTANs variegation locus of *Arabidopsis* defines a mitochondrial alternative oxidase homolog that functions during early chloroplast biogenesis. Plant Cell 11 (1999) 43-55.

[29] J. Barr, W.S. White, L. Chen, H. Bae, S. Rodermel, The GHOST terminal oxidase regulated developmental programming in tomato fruit. Plant Cell Environ. 27 (2004) 840–852.

[30] G.P. Rédei, Somatic instability caused by cysteine-sensitive gene in Arabidopsis. Science 139 (1963) 767-769.

[31] L. Houilles-Vernes, F. Rapaport, F.A. Wollman, J. Alric, X. Johnson, Plastid terminal oxidase 2 (PTOX2) is the major oxidase involved in chlororespiration in *Chlamydomonas*. Proc. Natl. Acad. Sci. U.S.A. 108 (2011) 20820-20825.

[32] M. Shimamura, *Marchantia polymorpha*: Taxonomy, phylogeny and morphology of a model system. Plant Cell Physiol. 57 (2016) 230-256.

[33] J.L. Bowman, T. Kohchi, K.T. Yamato, J. Jenkins, S. Shu, K. Ishizaki, S. Yamaoka, R. Nishihama, Y. Nakamura, F. Berger *et al.*,Insights into land plant evolution garnered from the *Marchantia polymorpha* genome. Cell 171 (2017) 287-304.

[34] R.C. Edgar, MUSCLE: multiple sequence alignment with high accuracy and high throughput. Nucleic Acids Res. 32 (2004) 1792-1797.

[35] S. Q. Le, O. Gascuel, An improved general amino acid replacement matrix. Mol. Biol. Evol. 25 (2008) 1307-1320.

[36] O. Gascuel, BIONJ: an improved version of the NJ algorithm based on a simple model of sequence data. Mol. Biol. Evol. 14 (1997) 685-695.

[37] S. Kumar, G. Stecher, M. Li, C. Knyaz, K. Tamura, MEGA X: Molecular evolutionary genetics analysis across computing platforms. Mol. Biol. Evol. 35 (2018) 1547-1549.

[38] O.L. Gamborg, R.A. Miller, K. Ojima, Nutrient requirements of suspension cultures of soybean root cells. Exp. Cell Res. 50 (1968) 151-158.

[39] S.S. Sugano, R. Nishihama, M. Shirakawa, J. Takagi, Y. Matsuda, S. Ishida *et al.*, Efficient CRISPR/Cas9-based genome editing and its application to conditional genetic analysis in *Marchantia polymorpha*. PLoS ONE 13 (2018) e0205117.

[40] A. Kubota, K. Ishizaki, M. Hosaka, T. Kohchi, Efficient agrobacterium-mediated transformation of the liverwort *Marchantia polymorpha* using regenerating thalli. Biosci. Biotechnol. Biochem. 77 (2013) 167-172.

[41] N.R. Baker, Chlorophyll fluorescence: a probe of photosynthesis *in vivo*. Annu. Rev. Plant Biol. 59 (2008) 89-113.

[42] J.P. Krall, G.E. Edwards, Relationship between photosystem II activity and CO_2 fixation in leaves. Physiol. Plant. 86 (1992) 180-187.

[43] C. Klughammer, U. Schreiber, An improved method, using saturating light pulses, for the determination of photosystem I quantum yield via $P700^+$-absorbance changes at 830 nm. Planta 192 (1994) 261-268.

[44] P.G. Falkowski, M.E. Katz, A.H. Knoll, A. Quigg, J.A. Raven, O. Schofield, F.J.R. Taylor, The evolution of modern eukaryotic phytoplankton. Science 305 (2004) 354-360.

[45] G. Shimakawa, K. Ishizaki, S. Tsukamoto, M. Tanaka, T. Sejima, C. Miyake, The liverwort, *Marchantia*, drives alternative electron flow using a flavodiiron protein to protect PSI. Plant Physiol. 173 (2017) 1636-1647.

[46] E. Derelle, C. Ferraz, S. Rombauts, P. Rouzé, A.Z. Worden, S. Robbens, F. Partensky, S. Degroeve, S. Echeynié, R. Cooke *et al.*,Genome analysis of the smallest free-living eukaryote Ostreococcus tauri unveils many unique features. Proc. Natl. Sci. U. S. A. 103 (2006) 11647-11652.

[47] A.E. McDonald, A.G. Ivanov, R. Bode, D.P. Maxwell, S.R. Rodermel, N.P. Hüner, Flexibility in photosynthetic electron transport: the physiological role of plastoquinol terminal oxidase (PTOX). Biochim. Biophys. Acta Bioenerg. 1807 (2011) 954-967.

[48] M. Iwai, K. Takizawa, R. Tokutsu, A. Okamuro, Y. Takahashi, J. Minagawa, Isolation of the elusive supercomplex that rives cyclic electron flow in photosynthesis. Nature 464 (2010) 1210-1213.

[49] J. Steinbeck, I. L. Ross, R. Rothnagel, P. Gäbelein, S. Schulze, N. Giles, R. Ali, R. Drysdale, E. Sierecki, Y. Gambin *et al*., Structure of a PSI-LHCI-cyt b_6f supercomplex

in *Chlamydomonas reinhardtii* promoting cyclic electron flow under anaerobic conditions. Proc. Natl. Acad. Sci. U. S. A. 115 (2018) 10517-10522.

[50] S. Bolte, E. Marcon, M. Jaunario, L. Moyet, M.T. Paternostre, M. Kuntz, A. Krieger-Liszkay, Dynamics of the localization of the plastid terminal oxidase PTOX inside the chloroplast. J. Exp. Bot. (2020) (in press) eraa074.

[51] T. Shiba, Y. Kido, K. Sakamoto, D. K. Inaoka, C. Tsuge, R. Tatsumi, G. Takahashi, E.O. Balogun, T. Nara, T. Aoki, *et al*., Structure of the trypanosome cyanide-insensitive alternative oxidase. Proc. Natl. Acad. Sci. U. S. A. 110 (2013) 4580-4585.

Figure legends

Fig. 1. Phylogenetic analysis of plastid terminal oxidase (PTOX) and alternative oxidase (AOX) isoforms in oxygenic phototrophs. (A) Typical primary structures of plant- and alga-type PTOX. TP, transit peptide; Fe-Fe, highly conserved region containing the catalytic site; C, C-terminal region; X, an extended region often observed in alga-type PTOX. (B) Phylogenetic tree of the evolutionary relationship between plastid terminal oxidase (PTOX) in oxygenic phototrophs. Each highly conserved region (Fe-Fe) was used for the alignment analysis to build the phylogenetic tree (Supplementary Material Fig. S2). Branch lengths correspond to the evolutionary distances. Organisms included in this phylogenetic analysis are cyanobacteria (*Gloeobacter violaceus*, *Anabaena cylindrica*, and *Nostoc* sp.), green algae (*Coccomyxa subellipsoidea*, *Ostreococcus tauri*, *Chlamydomonas reinhardtii*, and *Volvox carteriv*), the charophyte alga *Klebsormidium nitens*, the liverwort *Marchantia polymorpha*, ferns (*Azolla filiculoides* and *Salvinia cucullata*), angiosperms (*Arabidopsis thaliana*, *Oryza sativa*, *Zostera marina*, and *Zea mays*), the eustigmatophyte alga *Nannochloropsis oceanica*, diatoms (*Phaeodactylum tricornutum* and *Thalassiosira pseudonana*), and the red alga *Cyanidioschyzon merolae*. Alternative oxidase (AOX) in *Chlamydomonas reinhardtii* (AOX1) and *Arabidopsis thaliana* (AOX1A) are also included in the analysis.

Fig. 2. Response of chlorophyll fluorescence of wild type and mutants deficient in plastid terminal oxidase to illumination by blue actinic light (230 µmol photons $m^{-2}s^{-1}$). A: *M. polymorpha* wild type (Tak-1), B: Δ*ptoxa*, C: Δ*ptoxb*). Before the measurements, the plants were dark-adapted for 5 min. Dashed lines indicate the chlorophyll fluorescence levels before the first saturation flash. Blue bar indicates the duration of the actinic light. Measurements were conducted independently three times (biological replicates), and representative traces are shown.

Fig. 3. Typical trace of chlorophyll fluorescence change after switching off the actinic red light (400 µmol photons $m^{-2}s^{-1}$, 10 min) at 0 min in wild type (Tak-1; black) and the mutants deficient in plastid terminal oxidases a (Δ*ptoxa*; red) and b (Δ*ptoxb*; blue). Measurements were conducted independently three times (biological replicates), and representative traces are

shown. Dashed lines indicate the chlorophyll fluorescence levels prior to illumination. Application of far-red light suppressed the post illumination fluorescence rise as shown here for Δ*ptoxa* (green).

Fig. 4. Dependence of electron transport rate through PSII (A) and non-photochemical quenching (NPQ; B) on light intensity at steady-state photosynthesis (4 min after onset of actinic light) in *M. polymorpha* wild type (Tak-1; black) and the mutants deficient in plastid terminal oxidases a (Δ*ptoxa*; red) and b (Δ*ptoxb*; blue). Data are represented as the mean ± SD, $n = 3$ (biological replicates).

Fig. 5. Pigment content in thalli of *M. polymorpha* wild type (Tak-1; black) and the mutants deficient in plastid terminal oxidases a (Δ*ptoxa*; red) and b (Δ*ptoxb*; blue) determined by HPLC-UV measurement. Data are represented as the mean ± SD, $n = 3$ (technical replicates). Statistically significant differences (*) in Δ*ptoxb* compared to Tak-1 were determined by Student's *t*-test ($p < 0.05$).

Fig. 6. Oxidation of P700 in response to light in *M. polymorpha* wild type (Tak-1; black) and the mutants deficient in plastid terminal oxidases a (Δ*ptoxa*; red) and b (Δ*ptoxb*; blue). Red actinic light (500 µmol photons $m^{-2}s^{-1}$) and far-red light were given as indicated by red and white bars. Experiments were conducted independently three times (biological replicates), and the representative traces are shown. The maximum oxidation amplitude of P700 was determined by a saturation flash in at the end of the far-red light at 40 s.

Fig. 7. $P700^{+}$ re-reduction after illumination with far-red light in DCMU-treated thalli. Representative traces of *M. polymorpha* wild type (Tak-1, black) and the mutants deficient in plastid terminal oxidases a (Δ*ptoxa*; red) and b (Δ*ptoxb*; blue) are shown.

Fig. 8. PGR5 and NDH-B content in membranes fractions of *M. polymorpha* wild type (Tak-1) and the mutants deficient in plastid terminal oxidases a (Δ*ptoxa*) and b (Δ*ptoxb*) analyzed by SDS-PAGE and immunoblotting using specific antibodies. As loading controls, the signals

obtained with antibodies directed against RbcL(large subunit of Ribulose-1.5-bisphosphate carboxylase/oxygenase) and a part of the Coomassie stained gel are shown.

Figure 1

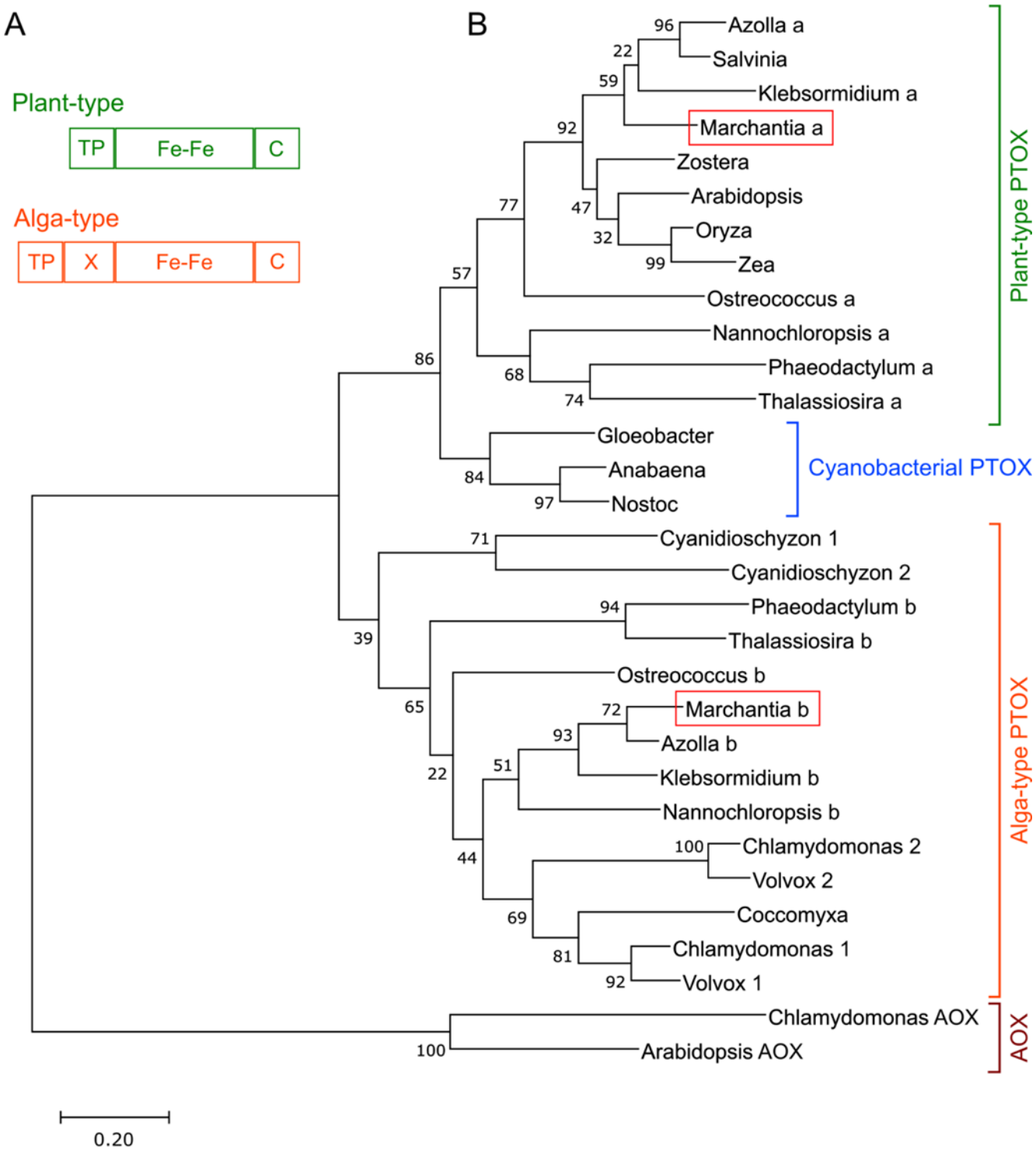
A
Plant-type
TP
Fe-Fe
C
Alga-type
TP
X
Fe-Fe
C
B
Azolla a
Salvinia
Klebsormidium a
Marchantia a
Zostera
Arabidopsis
Oryza
Zea
Ostreococcus a
Nannochloropsis a
Phaeodactylum a
Thalassiosira a
Gloeobacter
Anabaena
Nostoc
Cyanidioschyzon 1
Cyanidioschyzon 2
Phaeodactylum b
Thalassiosira b
Ostreococcus b
Marchantia b
Azolla b
Klebsormidium b
Nannochloropsis b
Chlamydomonas 2
Volvox 2
Coccomyxa
Chlamydomonas 1
Volvox 1
Chlamydomonas AOX
Arabidopsis AOX
96
22
59
92
77
47
32
99
57
86
68
74
84
97
71
94
39
65
72
93
51
22
44
100
69
81
92
100
Plant-type PTOX
Cyanobacterial PTOX
Alga-type PTOX
AOX
0.20

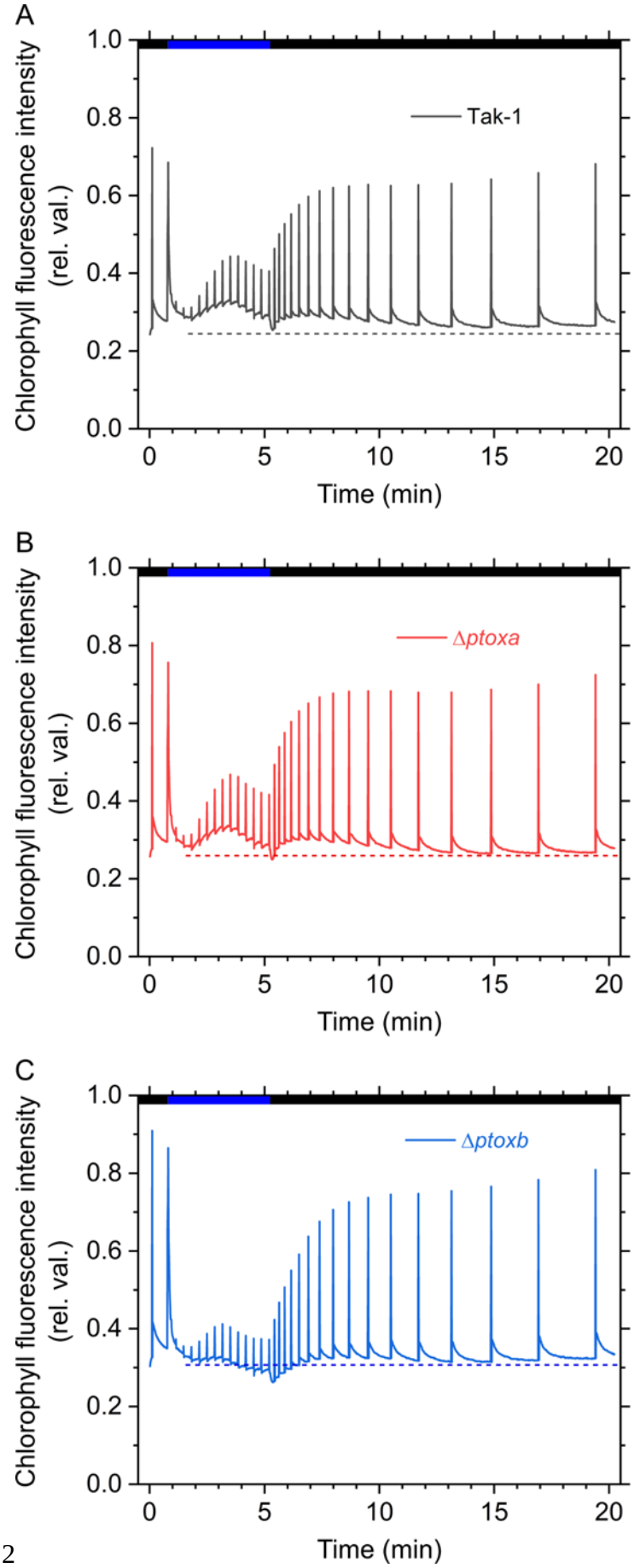
A
Chlorophyll fluorescence intensity (rel. val.)
1.0
0.8
0.6
0.4
0.2
0.0
Tak-1
0
5
10
15
20
Time (min)
B
Chlorophyll fluorescence intensity (rel. val.)
Δptoxa
Time (min)
C
Chlorophyll fluorescence intensity (rel. val.)
Δptoxb
Time (min)

Figure 2

Figure 3

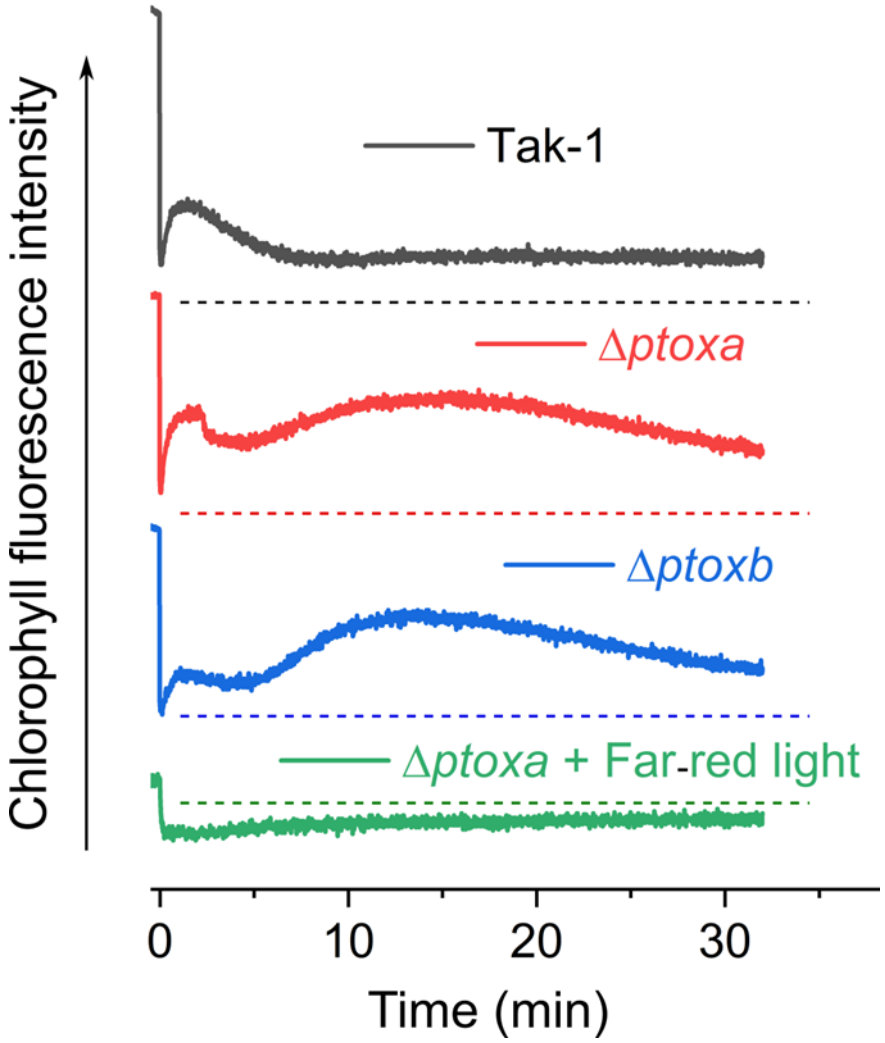
Chlorophyll fluorescence intensity
Tak-1
Δptoxa
Δptoxb
Δptoxa + Far-red light
0
10
20
30
Time (min)

Figure 4

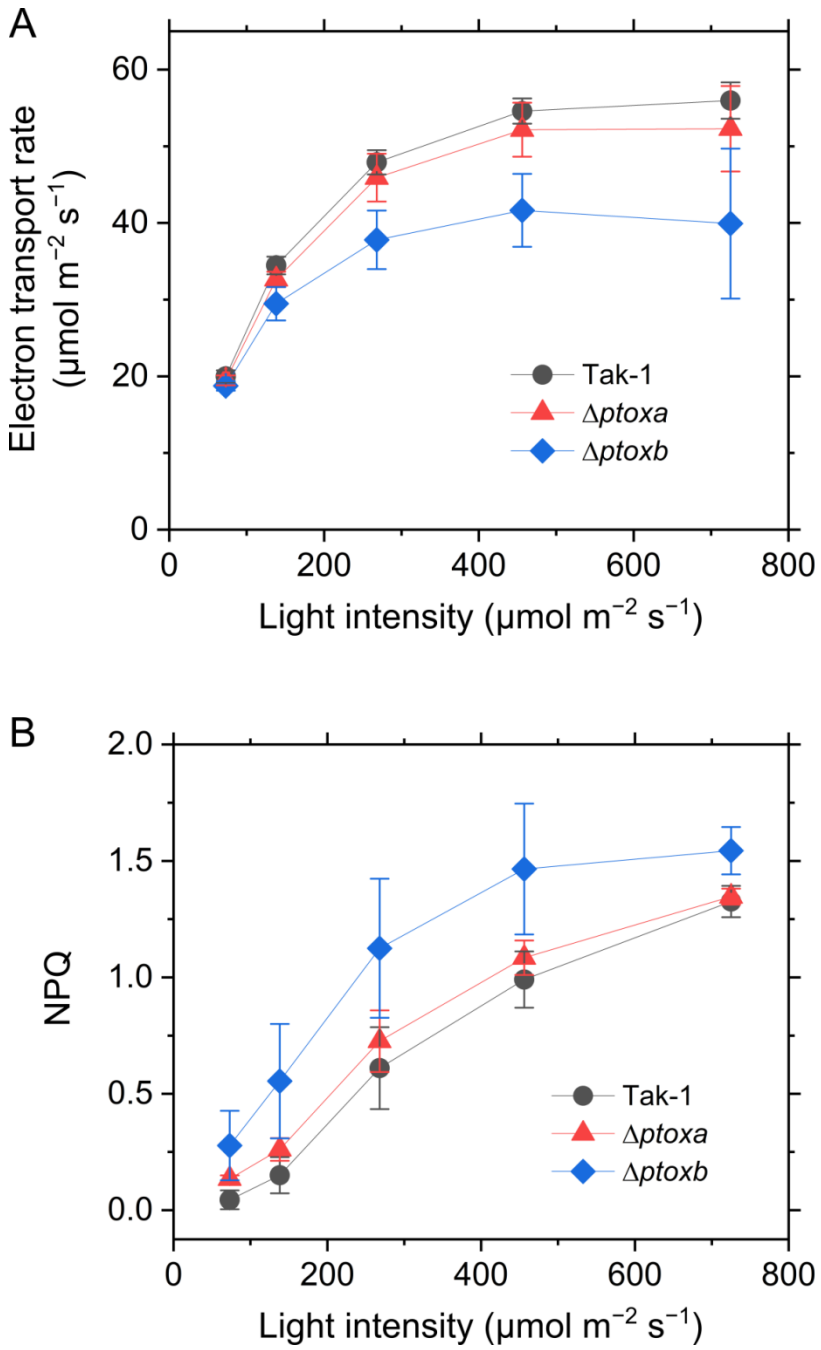
A
Electron transport rate (μmol m^{-2} s^{-1})
60
40
20
0
0
200
400
600
800
Light intensity (μmol m^{-2} s^{-1})
Tak-1
Δptoxa
Δptoxb
B
NPQ
2.0
1.5
1.0
0.5
0.0
0
200
400
600
800
Light intensity (μmol m^{-2} s^{-1})
Tak-1
Δptoxa
Δptoxb

Figure 5

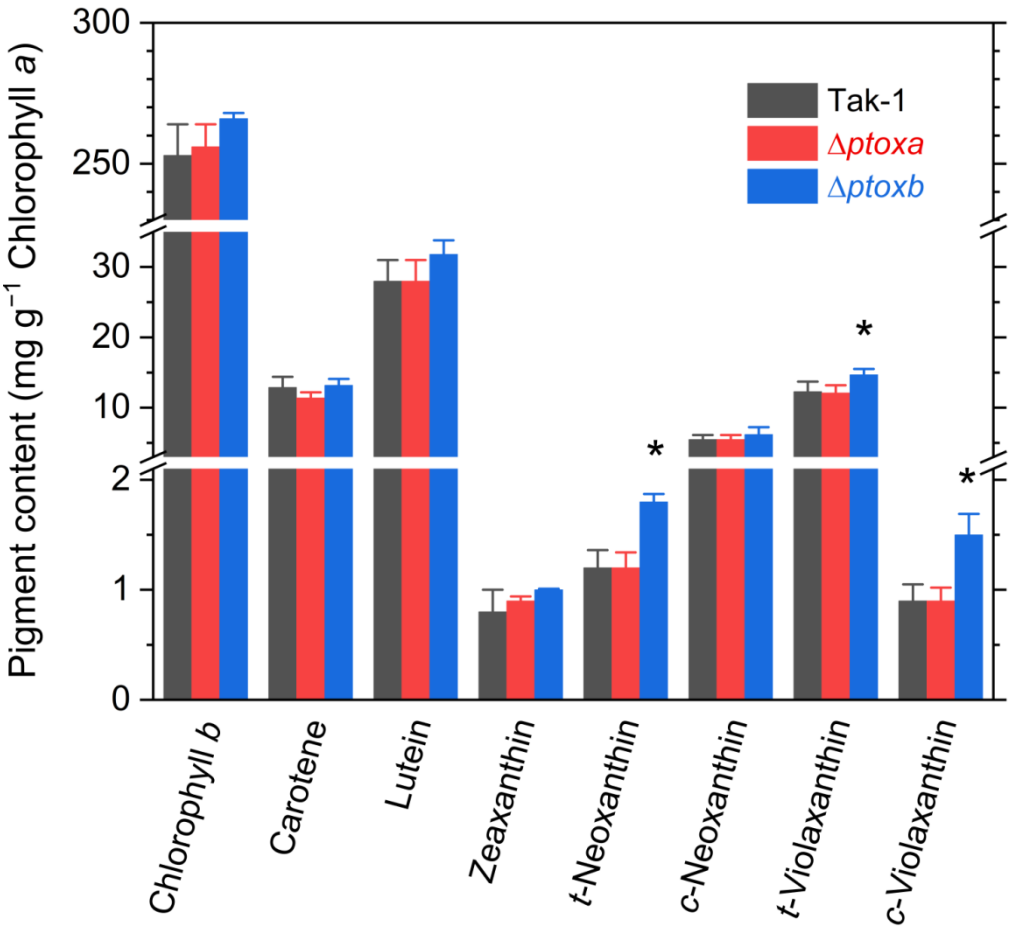
Pigment content (mg g^{-1} Chlorophyll *a*)
300
250
30
20
10
2
1
0
Tak-1
Δptoxa
Δptoxb
*
*
*
Chlorophyll *b*
Carotene
Lutein
Zeaxanthin
t-Neoxanthin
c-Neoxanthin
t-Violaxanthin
c-Violaxanthin

Figure 6

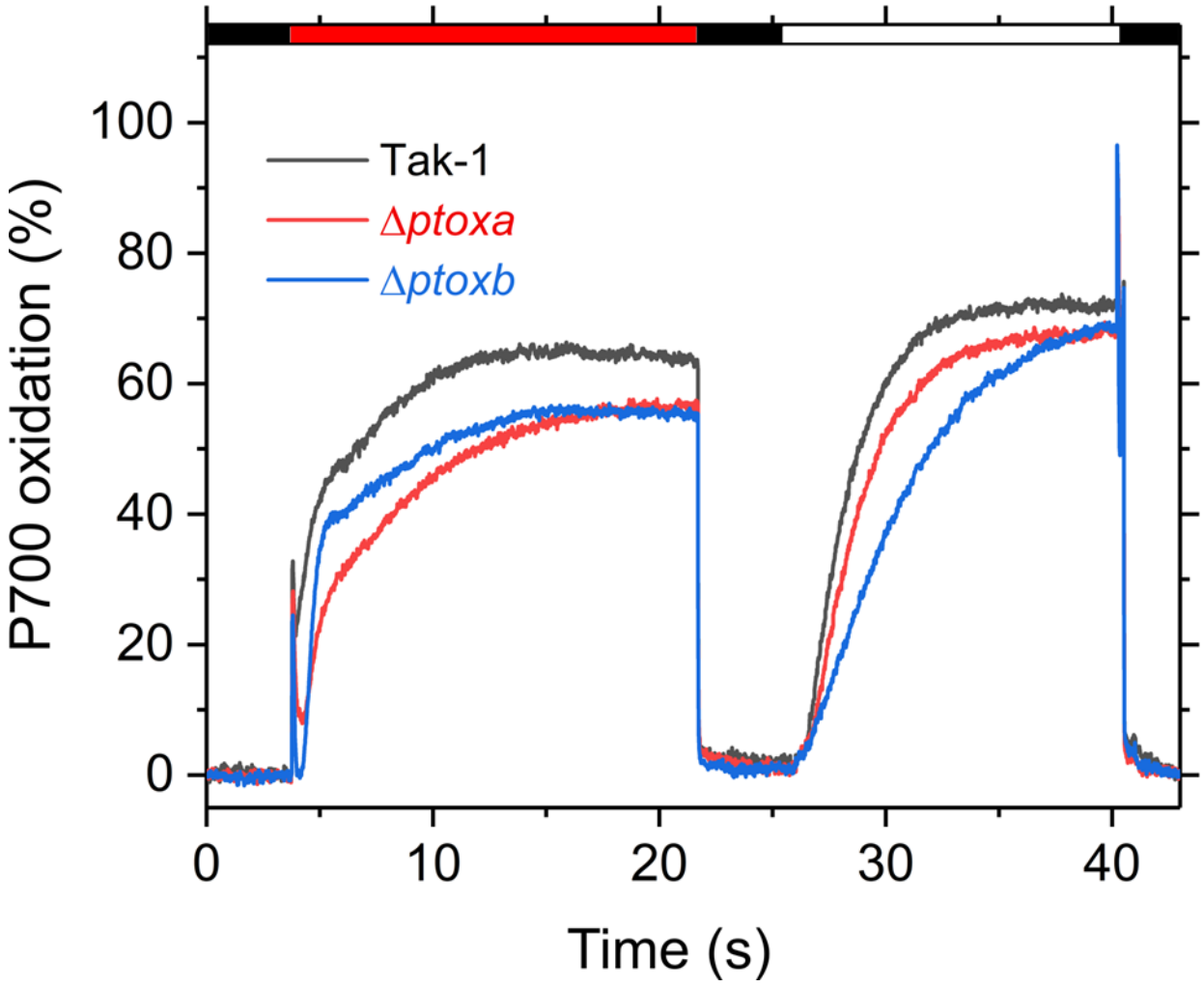
P700 oxidation (%)
100
80
60
40
20
0
0
10
20
30
40
Time (s)
Tak-1
Δptoxa
Δptoxb

Figure 7

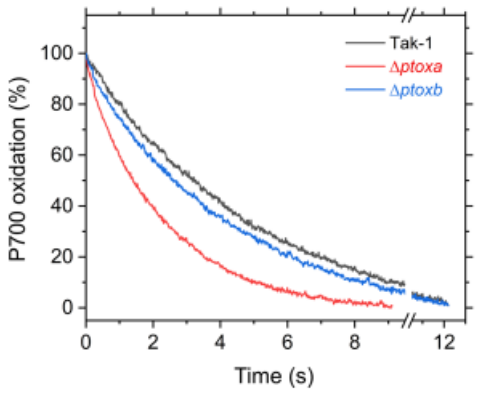

Figure 7

Figure 8